arXiv:1701.02318v1 [cond-mat.str-el] 9 Jan 2017

Elastic interactions and control of the Mott transition

G. G. Guzmán-Verri[1,2], R. T. Brierley[3], P. B. Littlewood[4,5]
[1] *Centro de Investigación en Ciencia e Ingeniería de Materiales and Escuela de Física, Universidad de Costa Rica, San José, Costa Rica 11501,*
[2] *Materials Science Division, Argonne National Laboratory, Argonne, Illinois, USA 60439,*
[3] *Department of Physics, Yale University, New Haven, Connecticut 06511, USA,*
[4] *Argonne National Laboratory, Argonne, Illinois, USA 60439, and*
[5] *James Franck Institute, University of Chicago, 929 E 57 St, Chicago, Illinois, USA 60637.*
(Dated: January 11, 2017)

Metal to insulator transitions (MIT) driven by strong electronic correlations are common in condensed matter systems, and are associated with some of the most remarkable collective phenomena in solids, including superconductivity and magnetism. Tuning and control of the transition holds the promise of novel, low power, ultrafast electronics[1,2], but the relative roles of doping, chemistry, elastic strain and other applied fields has made systematic understanding difficult to obtain. Here we point out that existing data on tuning of the MIT in perovskite transition metal oxides through ionic size effects provides evidence of systematic and large effects on the phase transition due to dynamical fluctuations of the elastic strain, which have been usually neglected. This is illustrated by a simple yet quantitative statistical mechanical calculation in a model that incorporates cooperative lattice distortions coupled to the electronic degrees of freedom. We reproduce the observed dependence of the transition temperature on cation radius in the well-studied manganite[3–8] and nickelate[9,10] materials. Since the elastic couplings are generically quite strong, these conclusions will broadly generalize to all MITs that couple to a change in lattice symmetry.

A large number of transition metal oxides (TMO) with the ABO_3 perovskite crystal structure allow tuning of the MIT by not only by the choice and average valence of the electronically active B ion (usually a $3d$ transition metal) but also by the size of the electronically inactive A ion (usually a rare earth or alkaline earth)[11–13]. This size effect can shift the transition temperature by hundreds of Kelvin, and the widely accepted explanation is that it is due to a reduction in the electron bandwidth as the bond bending induced by ionic size changes the orbital overlap[1,14]. However, the changes in bandwidth are typically less than a few percent[15], and it seems remarkable that a critical value of the ratio of interaction strength to bandwidth can be crossed in every $3d$ transition metal oxide, solely by varying the counterion.

Instead, we propose here that the observed dependence on the crystal structure arises from long-range, strain-mediated interactions, and that lattice fluctuations rather than electronic fluctuations tune the phase transition.

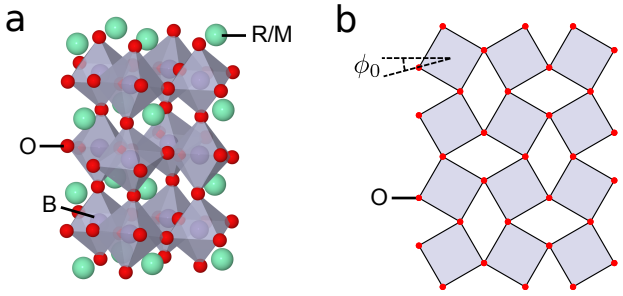

FIG. 1. (a) Perovskite lattice showing the tilts of the BO_6 (B=Mn,Ni) octahedra. R is a rare earch element such as La, Pr, Nd, and Sm; and M is an alkaline earth metal such as Ca, Sr, Ba. (b) 2D representation of the tilts used in our model where ϕ_0 is an initial equilibrium antiferrodistortive rotation.

The crystal structure of perovskite TMOs consists of corner-sharing oxygen octahedra surrounding the B transition metal ion, as shown in Fig. 1 (a). In general, the octahedra are tilted relative to their neighbors in an alternating pattern, and the tilt angle increases with smaller A-site cation radius r_A. The dramatic changes in the functional behavior of perovskites when varying the tilt angle have led to proposals to engineer material properties by manipulating the tilt angle using a combination of strain, doping and pressure[16]. In addition to variations of the atomic size, doping with A-site cations also introduces disorder in the cation size; careful distinction of the effects of doping and disorder for the manganites demonstrated that disorder reduces the transition temperature as effectively as does the average size change.[17]

Although purely electronic mechanisms to describe transition metal oxides are appealing in their theoretical simplicity, it is known that the strong electron-phonon coupling means that the effects of lattice distortions cannot be neglected, and this is particularly well studied in manganites and nickelates[18–20]. An electron that is localized by correlation effects in a unit cell will lower its energy further by the creation of a lattice distortion, which may be of different symmetry in different materials. In the nickelates this is a simple breathing distortion, and in the manganites a so-called Jahn-Teller distortion that lowers the cubic symmetry

of the octahedon. The competition between this potential energy gain and the kinetic energy gained by delocalization to form a metal gives rise to the complex MIT phenomena in these materials.

The corner-sharing constraint on the octahedra introduces compatibility conditions between distortions at different lattice sites; when integrating out the phonon degrees of freedom these yield highly anisotropic, long-range interactions[21,22]. Previous studies of phonon cooperativity in the manganites have demonstrated that they can explain the complex charge ordered phases and mesoscopic structures that have been observed in the manganites[23–26], and studied some effects of cooperative coupling on the transition[27–29]. However, these studies did not consider the effect of octahedral tilting on the long-range interaction of the distortions[25]. The purpose of this work is to study such effects, and in doing so, to construct a complete theory for cooperative elastic effects at a phase transition.

For illustration, we use a two-dimensional model of a transition metal perovskite, where we replace the octahedra by squares, as it is shown in Fig. 1 (b). Although the physics of bulk perovskites is three-dimensional, our approximation follows other studies of strain interactions in the manganites[25,30,31] and more generally[21,32–34] and significantly simplifies the geometry while still capturing the relevant physical behavior. At a lattice site $\mathbf{r}$, the squares can undergo the distortions shown in Fig. 2 (a): deviatoric/Jahn-Teller modes $T_{\mathbf{r}}$, dilatation/breathing modes $D_{\mathbf{r}}$, shear modes $S_{\mathbf{r}}$, and small rotations $R_{\mathbf{r}}$ of the squares from an initial equilibrium antiferrodistortive rotation ϕ_0, i.e., $\phi_{\mathbf{r}} = (-1)^{|\mathbf{r}|}\phi_0 + R_{\mathbf{r}}$. Assuming a harmonic energy penalty for creating distortions from an equilibrium configuration,

$$H = \sum_{\mathbf{r}} a_T T_{\mathbf{r}}^2 + a_D D_{\mathbf{r}}^2 + a_S S_{\mathbf{r}}^2, \qquad (1)$$

combined with the corner-sharing constraint, we can find the effective interaction $V_{\mathbf{r}\mathbf{r}'}(\phi_0)$ between different types of distortion (see supplement). a_D, a_S, and a_T are, respectively, the stiffness of breathing, shear, and Jahn-Teller distortions in a single, free octahedron and are independent of $\mathbf{r}$.

Fig. 3 shows that the interaction strength is reduced by an increase tilt angle for Jahn-Teller distortions. This occurs because in the tilted configuration it is possible for the distortion to be accomodated by additional rotations to the neighbouring sites, rather than changes in the shape. Characteristic strain responses of the lattice to a local Jahn-Teller distortion with and without rotations are shown in Fig. 2 (b).

Both manganites[35] and nickelates[36] undergo first-order transitions from a characteristic low temperature phase to a high-temperature polaronic phase. This suggests that the motion of conduction electrons through the lattice is associated with the creation of local structural distortions. When the distortion interaction $V_{\mathbf{r}\mathbf{r}'}(\phi_0)$ is

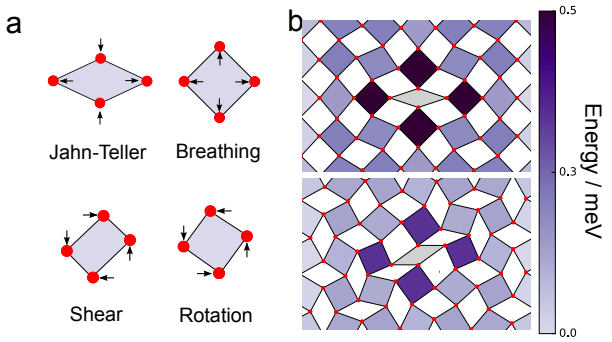

FIG. 2. (a) Lattice distortions considered in our model. (b) Strain responses of a lattice to a local Jahn-Teller distortion as a result of rotations. The color of each square indicates the strain energy associated with the local distortions of that square. The grey parallelogram at the centre has a Jahn-Teller distortion of fixed amplitude. Additional distortions on this site, such as shear, are allowed. Top: lattice with $\phi_0 = 0$. Bottom: lattice with $\phi_0 = 15^\circ$.

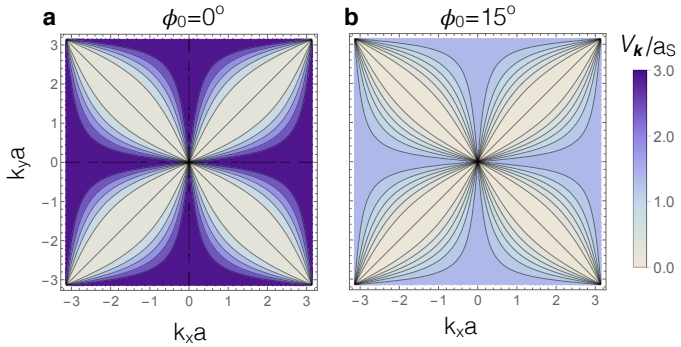

FIG. 3. Dependence of the effective elastic potential energy for Jahn Teller distortions on rotations in momentum space.

reduced by changes in ϕ_0, the high-temperature phase is favoured by a reduction in the polaron formation energy.[37] To study this behaviour, we use $V_{\mathbf{r}\mathbf{r}'}(\phi_0)$ to form a statistical mechanical model for the distortions in this high-temperature phase, with a Hamiltonian,

$$H = \sum_{\mathbf{r}} \left[\frac{1}{2}\Pi_{\mathbf{r}}^2 - \frac{\kappa}{2}Q_{\mathbf{r}}^2 + \frac{\gamma}{4}Q_{\mathbf{r}}^4\right] + \sum_{\mathbf{r}\mathbf{r}'} V_{\mathbf{r}\mathbf{r}'}(\phi_0) Q_{\mathbf{r}} Q_{\mathbf{r}'} - \sum_{\mathbf{r}} h_{\mathbf{r}} Q_{\mathbf{r}}, \qquad (2)$$

where $Q_{\mathbf{r}}$ is a Jahn-Teller (breathing) distortion for the manganites (nickelates) and $\Pi_{\mathbf{r}}$ its conjugate momentum. To model the the compositional disorder that arises in the manganites from chemical substitution of the alkaline earth element at the A site of the perovskite structure, we consider a linear coupling of the lattice distortions $Q_{\mathbf{r}}$ to a local quenched random distortion $h_{\mathbf{r}}$. We choose the $h_{\mathbf{r}}$'s to be normally distributed with mean $\bar{h}_{\mathbf{r}} = 0$ and variance Δ^2. The negative sign of the $Q_{\mathbf{r}}^2$ term describes the local tendency towards distortion due to the presence

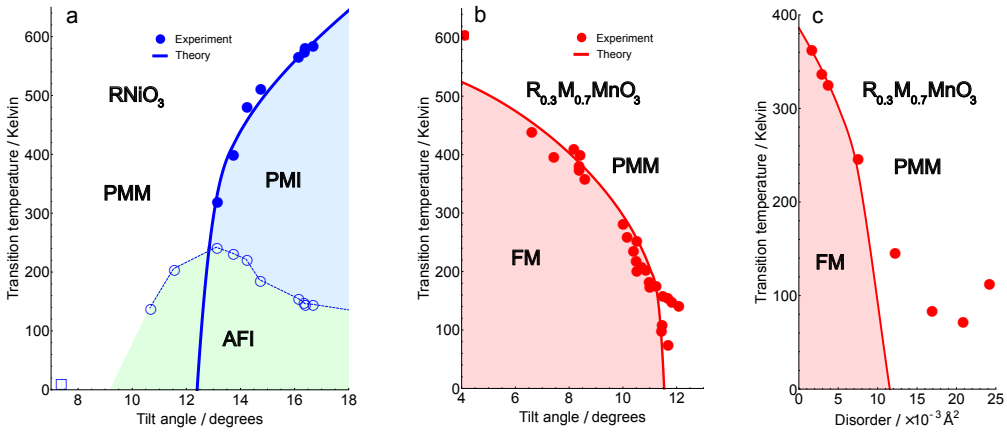

FIG. 4. Comparison between the results of our statistical mechanical calculation (solid lines) and experimental data for transitions in the nickelates and manganites. Fitted model parameters are given in Table S1 of the supplement. a: Comparison for the nickelates for the transition temperature as a function of octahedral tilt angle. Filled and open circles are experimental transition temperatures[10] for the paramagnetic insulator (PMI) and antiferromagnetic insulator (AFI) phases respectively. The extension of the green shading beyond the blue dashed line is an extrapolation. The open square denotes $LaNiO_3$, which is always in the high temperature polaronic, paramagnetic metal (PMM) phase. For the manganites, the comparison is made with results[17] (red circles) that separate the effect of tilt angle (b) and compositional disorder (c) on the transition from the paramagnetic, polaronic "bad metal" phase (PMM) to the ferromagnetic metal (FM) phase

of electrons.

Using a variational pair-distribution function that incorporates mean field behavior, Gaussian corrections to the thermal and quantum fluctuations, and disorder at the level of the replica method, (see supplement) we calculate the free energy of the system as a function of temperature, octahedral tilt angle ϕ_0 and the strength of disorder Δ^2. This approximate value is compared to a constant free energy $F_{\text{Low T}}$ associated with the low temperature phase to identify the location of the first-order phase transition, see Fig. 4. For the manganites, this phase corresponds to a ferromagnetic metal while for the nickelates it is a paramagnetic insulator. Despite the over-simplicity of the model, the relationship between tilt angle, disorder, and transition temperature is well reproduced. We do not attempt to describe the effects of the strain interactions on the MIT of the nickelates at low temperatures (see green region in Fig. 4 (a)), as its magnetic ordering is different from that of the insulating phase above it. Similarly for the manganites, at low enough temperatures the PMM phase becomes either charge-ordered or glassy, beyond our approximations.

Conclusions. In this paper we have outlined a systematic theory for the incorporation of long-range elastic couplings into a simplified statistical mechanical theory of Mott-like phase transitions, where the electronic contributions to the free energy are incorporated at the level of Landau theory. That these elastic interactions are explicitly relevant for the manganites and the nickelates is confirmed by the ability of such a theory to systematically explain size effects or tolerance factor variations which have already been documented. However the couplings, including their rough order-of-magnitude, are generic, and the ideas presented here will surely be relevant to other classes of materials such as the titanates[13], high temperature superconductors[38], ferroelectrics[39], and molecular fullerides[40].

At low enough temperatures one should surely take care of other low-energy degrees of freedom such as spin fluctuations and electronic quantum fluctuations which our model does not take into account. Nonetheless, the model we employ does generate a quantum critical point on account of elastic interactions alone. Moreover, the long range and anisotropy of these elastic couplings will modify the critical dynamics away from that arising from short-range models generated by purely electronic couplings.

Acknowledgements. Work at Argonne National Laboratory is supported by the U.S. Department of Energy, Office of Basic Energy Sciences under contract no. DE-AC02-06CH11357. RTB acknowledges the Yale Prize Postdoctoral Fellowship. Work at the University of Costa Rica is supported by the Vice-rectory for Research under the project no. 816-B5-222, GGGV and RTB acknowledge partial financial support from the Office of International Affairs at the University of Costa Rica.

Author contributions. PBL conceived the study; GGGV and RTB performed the calculations; all authors constructed the model, wrote the manuscript, discussed the results and implications at all stages.

Competing Interests. RTB is currently an editor at Nature Communications.

[1] M. Imada, A. Fujimori, and Y. Tokura, "Metal-insulator transitions," Rev. Mod. Phys. **70**, 1039–1263 (1998).

[2] Z. Yang, C. Ko, and S. Ramanathan, "Oxide Electronics Utilizing Ultrafast Metal-Insulator Transitions," Annual Review of Materials Research **41**, 337–367 (2011).

[3] J. M. D. Coey, M. Viret, and S. von Molnár, "Mixed-valence manganites," Advances in Physics **58**, 571–697 (2009).

[4] M. B. Salamon and M. Jaime, "The physics of manganites: Structure and transport," Rev. Mod. Phys. **73**, 583–628 (2001).

[5] E. Dagotto, T. Hotta, and A. Moreo, "Colossal magnetoresistant materials: the key role of phase separation," Physics Reports **344**, 1 – 153 (2001).

[6] N. D. Mathur and P. B. Littlewood, "The self-organised phases of manganites," Solid State Communications **119**, 271 – 280 (2001).

[7] N. D. Mathur and P. B Littlewood, "Mesoscopic Texture in Manganites," Physics Today **56**, 25 (2003).

[8] Y. Tokura, "Critical features of colossal magnetoresistive manganites," Reports on Progress in Physics **69**, 797 (2006).

[9] M. L. Medarde, "Structural, magnetic and electronic properties of $RNiO_3$ perovskites (R = rare earth)," Journal of Physics: Condensed Matter **9**, 1679 (1997).

[10] G. Catalan, "Progress in perovskite nickelate research," Phase Transitions **81**, 729–749 (2008).

[11] J. B. Torrance, P. Lacorre, A. I. Nazzal, E. J. Ansaldo, and Ch. Niedermayer, "Systematic study of insulator-metal transitions in perovskites $RNiO_3$ (R=Pr,Nd,Sm,Eu) due to closing of charge-transfer gap," Phys. Rev. B **45**, 8209–8212 (1992).

[12] H. Y. Hwang, S-W. Cheong, P. G. Radaelli, M. Marezio, and B. Batlogg, "Lattice effects on the magnetoresistance in doped $LaMnO_3$," Phys. Rev. Lett. **75**, 914–917 (1995).

[13] T. Katsufuji, Y. Taguchi, and Y. Tokura, "Transport and magnetic properties of a Mott-Hubbard system whose bandwidth and band filling are both controllable: $R_{1-x}Ca_xTiO_{3+y/2}$," Phys. Rev. B **56**, 10145–10153 (1997).

[14] A. Fujimori, "Electronic structure of metallic oxides: Band-gap closure and valence control," J. Phys. Chem. Solids **53**, 1595 (1992).

[15] P. G. Radaelli, G. Iannone, M. Marezio, H. Y. Hwang, S-W. Cheong, J. D. Jorgensen, and D. N. Argyriou, "Structural effects on the magnetic and transport properties of perovskite $A_{1-x}A'_xMnO_3$ (x = 0.25, 0.30)," Phys. Rev. B **56**, 8265–8276 (1997).

[16] J. M. Rondinelli, S. J. May, and J. W. Freeland, "Control of octahedral connectivity in perovskite oxide heterostructures: An emerging route to multifunctional materials discovery," MRS Bulletin **37**, 261–270 (2012).

[17] L. M. Rodriguez-Martinez and J. P. Attfield, "Cation disorder and size effects in magnetoresistive manganese oxide perovskites," Phys. Rev. B **54**, R15622–R15625 (1996).

[18] A. J. Millis, P. B. Littlewood, and B. I. Shraiman, "Double exchange alone does not explain the resistivity of $La_{1-x}Sr_xMnO_3$," Phys. Rev. Lett. **74**, 5144–5147 (1995).

[19] H. Röder, Jun Zang, and A. R. Bishop, "Lattice effects in the colossal-magnetoresistance manganites," Phys. Rev. Lett. **76**, 1356–1359 (1996).

[20] S. Johnston, A. Mukherjee, I. Elfimov, M. Berciu, and G. A. Sawatzky, "Charge Disproportionation without Charge Transfer in the Rare-Earth-Element Nickelates as a Possible Mechanism for the Metal-Insulator Transition," Physical Review Letters **112**, 106404 (2014).

[21] S. Kartha, J. A. Krumhansl, J. P. Sethna, and L. K. Wickham, "Disorder-driven pretransitional tweed pattern in martensitic transformations," Phys. Rev. B **52**, 803 (1995).

[22] M. Porta, T. Castán, P. Lloveras, T. Lookman, A. Saxena, and S. R. Shenoy, "Interfaces in ferroelastics: Fringing fields, microstructure, and size and shape effects," Phys. Rev. B **79**, 214117 (2009).

[23] K. I. Kugel and D. I. Khomskii, "The Jahn-Teller effect and magnetism: transition metal compounds," Soviet Physics Uspekhi **25**, 231 (1982).

[24] D. I. Khomskii and K. I. Kugel, "Why stripes? Spontaneous formation of inhomogeneous structures due to elastic interactions," EPL (Europhysics Letters) **55**, 208 (2001).

[25] K. H. Ahn, T. Lookman, and A. R. Bishop, "Strain-induced metal-insulator phase coexistance in perovskite manganites," Nature **428**, 401 (2004).

[26] T. F. Seman, K. H. Ahn, T. Lookman, A. Saxena, A. R. Bishop, and P. B. Littlewood, "Effects of rare-earth ion size on the stability of the coherent Jahn-Teller distortions in undoped perovskite manganites," Phys. Rev. B **86**, 184106 (2012).

[27] A. J. Millis, "Cooperative Jahn-Teller effect and electron-phonon coupling in $La_{1-x}A_xMnO_3$," Physical Review B **53**, 8434–8441 (1996).

[28] T. Hotta, S. Yunoki, M. Mayr, and E. Dagotto, "A-type antiferromagnetic and C-type orbital-ordered states in $lamno_3$ using cooperative Jahn-Teller phonons," Physical Review B **60**, R15009–R15012 (1999).

[29] J. Burgy, A. Moreo, and E. Dagotto, "Relevance of cooperative lattice effects and stress fields in phase-separation theories for CMR manganites," Phys. Rev. Lett. **92**, 097202 (2004).

[30] A. Saxena, T. Castn, A. Planes, M. Porta, Y. Kishi, T. A. Lograsso, D. Viehland, M. Wuttig, and M. De Graef, "Origin of Magnetic and Magnetoelastic Tweedlike Precursor Modulations in Ferroic Materials," Physical Review Letters **92**, 197203 (2004).

[31] S. Nambu and D. A. Sagala, "Domain formation and elastic long-range interaction in ferroelectric perovskites," Physical Review B **50**, 5838 (1994).

[32] A. M. Bratkovsky, S. C. Marais, V. Heine, and E. K. H. Salje, "The theory of fluctuations and texture embryos in structural phase transitions mediated by strain," Journal of Physics: Condensed Matter **6**, 3679 (1994).

[33] S. Shenoy, T. Lookman, A. Saxena, and A. Bishop, "Martensitic textures: Multiscale consequences of elastic compatibility," Physical Review B **60**, R12537–R12541 (1999).

[34] K. Bhattacharya, S. Conti, G. Zanzotto, and J. Zimmer, "Crystal symmetry and the reversibility of martensitic transformations," Nature **428**, 55–59 (2004).

[35] Ch. Jooss, L. Wu, T. Beetz, R. F. Klie, M. Beleggia, M. A. Schofield, S. Schramm, J. Hoffmann, and Y. Zhu,

"Polaron melting and ordering as key mechanisms for colossal resistance effects in manganites," Proceedings of the National Academy of Sciences **104**, 13597–13602 (2007).

[36] R. Jaramillo, D. Ha Sieu, D. M. Silevitch, and S. Ramanathan, "Origins of bad-metal conductivity and the insulator-metal transition in the rare-earth nickelates," Nat. Phys. **10**, 304 (2015).

[37] Despina Louca, T. Egami, W. Dmowski, and J. F. Mitchell, "Structural effect on colossal magnetoresistivity in manganites: Bond versus band," Phys. Rev. B **64**, 180403 (2001).

[38] J. P. Attfield, A. L. Kharlanov, and J. A. McAllister, "Cation effects in doped La_2CuO_4 superconductors," Nature **394**, 157 (1998).

[39] P. V. Balachandran, S. R. Broderick, and K. Rajan, "Identifying the inorganic gene for high-temperature piezoelectric perovskites through statistical learning," Proc. R. Soc. A **467**, 2271–2290 (2011).

[40] R. H. Zadik, Y. Takabayashi, G. Klupp, R. H. Colman, A. Y. Ganin, A. Potočnik, P. Jeglič, D. Arčon, P. Matus, K. Kamarás, Y. Kasahara, Y. Iwasa, A. N. Fitch, Y. Ohishi, G. Garbarino, K. Kato, M. J. Rosseinsky, and K. Prassides, "Optimized unconventional superconductivity in a molecular Jahn-Teller metal," Science Advances **1** (2015), 10.1126/sciadv.1500059.

Supplemental Information- Elastic interactions and control of the Mott transition

The purpose of this SI is to present details about the derivation of the elastic interactions, our model Hamiltonian, its solution, and additional results.

I. DISTORTION INTERACTION

We consider a two-dimensional model of a perovskite, consisting of corner-coupled quadrilaterals that are the analogues of the three-dimensional oxygen octahedra. Similar two-dimensional models have been used in earlier studies of strain in functional materials, including the manganites[S1,S2]. The displacements of the corners of the quadrilateral centred at a position $\mathbf{r}$ from their initial positions are the vectors $\mathbf{t_r}$, $\mathbf{u_r}$, $\mathbf{v_r}$ and $\mathbf{w_r}$ (see Fig. S1). To simplify the analysis, we assume that the allowed (i.e. low energy) configurations of the quadrilaterals are parallelograms, so that

$$\mathbf{t_r} - \mathbf{w_r} = \mathbf{u_r} - \mathbf{v_r}. \tag{S1}$$

This corresponds to assuming there is infinite energy cost associated with "shuffle" modes within the a quadrilateral[S3]. With this assumption, deviations from an initial configuration can be described in terms of four degrees of freedom: a rotation and three "strains" (see Fig. S1(a) of the main text), $D_\mathbf{r}$ (dilatation/breathing modes), $S_\mathbf{r}$ (shear modes) and $T_\mathbf{r}$ (deviatoric/Jahn-Teller modes). We assume that rotations of the squares from an initial equilibrium antiferrodistortive rotation ϕ_0 are small, writing $\phi_\mathbf{r} = (-1)^{|\mathbf{r}|}\phi_0 + R_\mathbf{r}$ and all equations involving $R_\mathbf{r}$ can be linearized. We take the following simple form for the elastic energy,

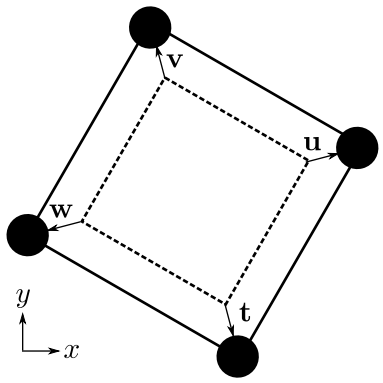

FIG. S1. A quadrilaterial altered from its equilibrium state (dashed) by a breathing distortion. The corner atoms displaced by displacement vectors $\mathbf{t_r}$, $\mathbf{u_r}$, $\mathbf{v_r}$ and $\mathbf{w_r}$.

$$H = \sum_\mathbf{r} a_T T_\mathbf{r}^2 + a_D D_\mathbf{r}^2 + a_S S_\mathbf{r}^2, \tag{S2}$$

where a_i is the energy penalty for the corresponding distortion of a free octahedron. Note that we make the approximation that the cost of rotations is small enough that it can be negelected. Such a term should exist in order for there to be a state with a non-zero ϕ_0, as observed in experiment. In the perovskite model, the constraint that the squares share corners means that $\mathbf{t_r} = \mathbf{v_{r-y}}$ and $\mathbf{w_r} = \mathbf{u_{r-x}}$. These constraints reduce the number of degrees of freedom per site to 2. Distortions of neighboring squares are coupled and as a result the energy given in Eq. (S2) actually describes a system with long-range strain interactions.

We can find the constraint equations in terms of the rotation and strain degrees of freedom by expressing them in terms of the atom positions $\mathbf{t_r}$, $\mathbf{u_r}$, $\mathbf{v_r}$ and $\mathbf{w_r}$, then using the corner-sharing constraint to eliminate the positions. We assume that rotations of the squares from an initial equilibrium antiferrodistortive rotation ϕ_0 are small, writing

$\phi_{\mathbf{r}} = (-1)^{|\mathbf{r}|}\phi_0 + R_{\mathbf{r}}$. Then we assume that the equation for $R_{\mathbf{r}}$ is linear and our equations are,

$$R_{\mathbf{r}} = \cos\phi_0(u^y_{\mathbf{r}} - u^y_{\mathbf{r}-\mathbf{n}_x} - v^x_{\mathbf{r}} + v^x_{\mathbf{r}-\mathbf{n}_y}) - (-1)^{|\mathbf{r}|}\sin\phi_0(u^x_{\mathbf{r}} - u^x_{\mathbf{r}-\mathbf{n}_x} + v^y_{\mathbf{r}} - v^y_{\mathbf{r}-\mathbf{n}_y}), \tag{S3a}$$

$$S_{\mathbf{r}} = \cos\phi_0(u^y_{\mathbf{r}} - u^y_{\mathbf{r}-\mathbf{n}_x} + v^x_{\mathbf{r}} - v^x_{\mathbf{r}-\mathbf{n}_y}) - (-1)^{|\mathbf{r}|}\sin\phi_0(u^x_{\mathbf{r}} - u^x_{\mathbf{r}-\mathbf{n}_x} - v^y_{\mathbf{r}} + v^y_{\mathbf{r}-\mathbf{n}_y}), \tag{S3b}$$

$$T_{\mathbf{r}} = \cos\phi_0(u^x_{\mathbf{r}} - u^x_{\mathbf{r}-\mathbf{n}_x} - v^y_{\mathbf{r}} + v^y_{\mathbf{r}-\mathbf{n}_y}) + (-1)^{|\mathbf{r}|}\sin\phi_0(u^y_{\mathbf{r}} - u^y_{\mathbf{r}-\mathbf{n}_x} + v^x_{\mathbf{r}} - v^x_{\mathbf{r}-\mathbf{n}_y}), \tag{S3c}$$

$$D_{\mathbf{r}} = \cos\phi_0(u^x_{\mathbf{r}} - u^x_{\mathbf{r}-\mathbf{n}_x} + v^y_{\mathbf{r}} - v^y_{\mathbf{r}-\mathbf{n}_y}) + (-1)^{|\mathbf{r}|}\sin\phi_0(u^y_{\mathbf{r}} - u^y_{\mathbf{r}-\mathbf{n}_x} - v^x_{\mathbf{r}} + v^x_{\mathbf{r}-\mathbf{n}_y}), \tag{S3d}$$

where we have used the convention $\mathbf{r}_{\mathbf{r}} = (r^x_{\mathbf{r}}, r^y_{\mathbf{r}})$ for the vector components.

After Fourier transformation, the parallelogram condition Eq. (S1), combined with the corner sharing constraint, can be written as,

$$(1 + e^{ik_xL})\mathbf{u}_{\mathbf{k}} = (1 + e^{ik_yL})\mathbf{v}_{\mathbf{k}},$$

where L is lattice spacing in the equilibrium configuration. Using this relationship, the Fourier transform of Eq. (S3) is,

$$R_{\mathbf{k}} = 2i\left(1 + e^{ik_xL}\right)\left[\cos\phi_0\left(t_xu^y_{\mathbf{k}} - t_yu^x_{\mathbf{k}}\right) - \frac{\sin\phi_0}{t_y}\left(t_yu^x_{\mathbf{M}-\mathbf{k}} + t_xu^y_{\mathbf{M}-\mathbf{k}}\right)\right],$$

$$S_{\mathbf{k}} = 2i\left(1 + e^{ik_xL}\right)\left[\cos\phi_0\left(t_xu^y_{\mathbf{k}} + t_yu^x_{\mathbf{k}}\right) - \frac{\sin\phi_0}{t_y}\left(t_yu^x_{\mathbf{M}-\mathbf{k}} - t_xu^y_{\mathbf{M}-\mathbf{k}}\right)\right],$$

$$T_{\mathbf{k}} = 2i\left(1 + e^{ik_xL}\right)\left[\cos\phi_0\left(t_xu^x_{\mathbf{k}} - t_yu^y_{\mathbf{k}}\right) + \frac{\sin\phi_0}{t_y}\left(t_yu^y_{\mathbf{M}-\mathbf{k}} + t_xu^x_{\mathbf{M}-\mathbf{k}}\right)\right],$$

$$D_{\mathbf{k}} = 2i\left(1 + e^{ik_xL}\right)\left[\cos\phi_0\left(t_xu^x_{\mathbf{k}} + t_yu^y_{\mathbf{k}}\right) + \frac{\sin\phi_0}{t_y}\left(t_yu^y_{\mathbf{M}-\mathbf{k}} - t_xu^x_{\mathbf{M}-\mathbf{k}}\right)\right],$$

where $\mathbf{M} = (\pi, \pi)$ is the wavevector of the antiferrodistortive order and we have defined,

$$t_i = \tan\frac{k_iL}{2}.$$

Finally we can eliminate $\mathbf{u}_{\mathbf{k}}$ to obtain a set of (discrete) compatibility conditions,

$$\begin{aligned} R_{\mathbf{k}} = f_{\mathbf{k}}\Big\{&4t_xt_y\left[-(t_x^2 + t_y^2)T_{\mathbf{k}} + \cos 2\phi_0(t_x^2 - t_y^2)D_{\mathbf{k}}\right] \\ &+2\sin 2\phi_0(t_x^2 - t_y^2)\left[(t_x^2 + t_y^2)T_{\mathbf{M}-\mathbf{k}} + \cos 2\phi_0(t_x^2 - t_y^2)D_{\mathbf{M}-\mathbf{k}}\right]\Big\}, \end{aligned} \tag{S4}$$

$$\begin{aligned} S_{\mathbf{k}} = f_{\mathbf{k}}\Big\{&4t_xt_y\left[(t_x^2 + t_y^2)D_{\mathbf{k}} - \cos 2\phi_0(t_x^2 - t_y^2)T_{\mathbf{k}}\right] \\ &+2\sin 2\phi_0(t_x^2 - t_y^2)\left[(t_x^2 + t_y^2)D_{\mathbf{M}-\mathbf{k}} + \cos 2\phi_0(t_x^2 - t_y^2)T_{\mathbf{M}-\mathbf{k}}\right]\Big\}. \end{aligned} \tag{S5}$$

where,

$$f_{\mathbf{k}} = \frac{1}{8t_x^2t_y^2 + 2(t_x^2 - t_y^2)^2\sin^2 2\phi_0}.$$

Note that these relationships have singular behavior when the k_i approach 0 or π. In particular, there is no relationship between the fields when $\mathbf{k} = \mathbf{0}$ or $\mathbf{M}$, i.e. the cases of homogeneous and antiferrodistortive deformations; each strain field is a separate degree of freedom in these cases[S4].

In the long-wavelength limit, $t_x \to k_xL/2$ and when $\phi_0 = 0$ we can write Eq. (S5) as,

$$(k_x^2 + k_y^2)D_{\mathbf{k}} - 2k_xk_yS_{\mathbf{k}} - (k_x^2 - k_y^2)T_{\mathbf{k}} = 0,$$

which is the Fourier transform of the usual two-dimensional compatibility relation[S5].

We can now substitute Eq. (S5) into the Fourier transform of Eq. (S2) to find the result without separate constraints:

$$F = \sum_{\mathbf{k}=\mathbf{0}}^{(\pi,\pi)} \left[a_T + 2a_S f_{\mathbf{k}}(t_x^2 - t_y^2)^2 \cos^2 2\phi_0\right] |T_{\mathbf{k}}|^2 + \left[a_D + 2a_S f_{\mathbf{k}}(t_x^2 + t_y^2)^2\right] |D_{\mathbf{k}}|^2 \\ - 2a_S f_{\mathbf{k}}(t_x^4 - t_y^4) \cos 2\phi_0 (D_{\mathbf{k}}^* T_{\mathbf{k}} + \text{h.c.}). \tag{S6}$$

In deriving this result, we have made use of the fact that the summation is over the entire Brillouin zone of the undistorted, $\phi_0 = 0$, system and the property that $t_i \to 1/t_i$ when $\mathbf{k} \to \mathbf{M} - \mathbf{k}$. Since each power of t_i appears equally often in the numerators and denominators of Eq. (S6), this relationship effectively means that $(t_x^2 - t_y^2) \to -(t_x^2 - t_y^2)$ under the change of wavevector, producing cancellations between terms that would otherwise couple different wavevectors.

To obtain the static interaction between the single strain fields $T_{\mathbf{k}}$ or $D_{\mathbf{k}}$, we can minimize the energy with respect to the other field:

$$D_{\mathbf{k}} = \frac{2a_S f_{\mathbf{k}}(t_x^4 - t_y^4)\cos 2\phi_0}{a_D + 2a_S f_{\mathbf{k}}(t_x^2 + t_y^2)^2} T_{\mathbf{k}}, \quad \text{or} \quad T_{\mathbf{k}} = \frac{2a_S f_{\mathbf{k}}(t_x^4 - t_y^4)\cos 2\phi_0}{a_T + 2a_S f_{\mathbf{k}}(t_x^2 - t_y^2)^2 \cos^2 2\phi_0} D_{\mathbf{k}}.$$

Substituting these results into Eq. (S6), we obtain the energy for a single strain field, including the long-range interaction term,

$$H_T = \sum_{\mathbf{k}} \left\{ a_T + \frac{a_D a_S \cos^2 2\phi_0 (t_x^2 - t_y^2)^2}{4a_D t_x^2 t_y^2 + a_S(t_x^2 + t_y^2)^2 + a_D(t_x^2 - t_y^2)^2 \sin^2 2\phi_0} \right\} |T_{\mathbf{k}}|^2 \tag{S7a}$$

$$H_D = \sum_{\mathbf{k}} \left\{ a_D + \frac{a_S a_T (t_x^2 + t_y^2)^2}{4a_T t_x^2 t_y^2 + a_S(t_x^2 - t_y^2)^2 + (a_T - a_S)(t_x^2 - t_y^2)^2 \sin^2 2\phi_0} \right\} |D_{\mathbf{k}}|^2. \tag{S7b}$$

These strain interactions are highly anisotropic, as it is shown, respectively, in Figs. 3 and S2 for H_T and H_D and non-analytic; as $|\mathbf{k}| \to 0$, the value of the potential depends on the direction of $\mathbf{k}$. The potential vanishes for (anti-)ferrodistortive perturbations, corresponding to $\mathbf{k} = 0$ ($\mathbf{k} = \mathbf{M} = (\pi, \pi)$), as the different distortion modes are uncoupled at those wavevectors. This implies a discontinuity at $\mathbf{k} = \mathbf{M}$, which arises from our assumption that the distortions in Fig. S1 are the only distortions, neglecting the shuffle modes for the octahedra.[S6] However, as long as such modes are significantly stiffer than the high-symmetry modes we do consider, this should not be an important approximation. In the long-wavelength limit and no rotations, $V_{\mathbf{k}}(\phi_0 = 0)$ for the manganites matches that of previous work.[S5,S7]

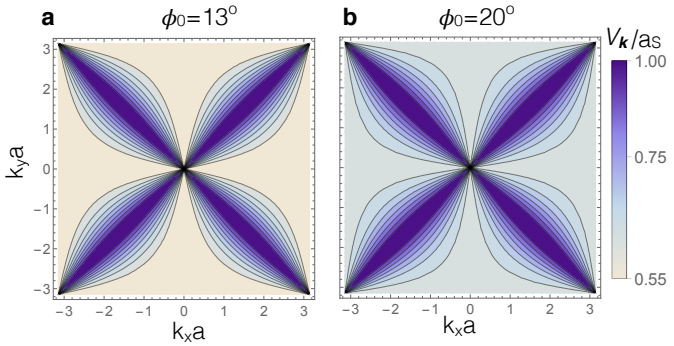

FIG. S2. Dependence of the effective elastic potential energy on rotations in momentum space for the nickelates.

II. STATISTICAL MECHANICAL MODEL

When an electron is present on a lattice site, there is an energetic benefit to creating a lattice distortion. To model this, we consider the following model Hamiltonian on a square lattice,

$$H = \sum_{\mathbf{r}} \left[\frac{1}{2}\Pi_{\mathbf{r}}^2 - \frac{\kappa}{2} Q_{\mathbf{r}}^2 + \frac{\gamma}{4} Q_{\mathbf{r}}^4 \right] + \sum_{\mathbf{r}\mathbf{r}'} V_{\mathbf{r}\mathbf{r}'}(\phi_0) Q_{\mathbf{r}} Q_{\mathbf{r}'} - \sum_{\mathbf{r}} h_{\mathbf{r}} Q_{\mathbf{r}},$$

where $Q_{\mathbf{r}}$ is a lattice distortion at site $\mathbf{r}$ associated with the strain modes and $\Pi_{\mathbf{r}}$ its conjugate momentum. $V_{\mathbf{r}\mathbf{r}'}(\phi_0)$ is a strain coupling with Fourier component $V_{\mathbf{k}}(\phi_0)$ given in Eq. (S7). The $h_{\mathbf{r}}$'s are local quenched random distortions that arise from chemical substitution of the alkaline earth element at the A site of the perovskite structure. We choose the $h_{\mathbf{r}}$s to be independent random variables with a Gaussian distribution with zero mean and variance Δ^2.

To study the statistical mechanics of the the model Hamiltonian (2) and handle compositional disorder, we use the variational method developed in Ref. [S8]. This method includes leading correlations beyond the mean-field approximation as well as disorder averaging at the level of a simple replica theory. In the absence of disorder, the results are equivalent to those of the standard self-consistent phonon approximation. The method is described in detail in Ref. [S8], however, we briefly described it here for the sake of completeness.

We consider a trial pair-probability distribution, $\rho^{tr} = (Z^{tr})^{-1} e^{-\beta H^{tr}}$, where H^{tr} is the Hamiltonian of coupled harmonic oscillators in a random field, $H^{tr} = \sum_{\mathbf{r}} \frac{1}{2}\Pi_{\mathbf{r}}^2 + \frac{1}{2}\sum_{\mathbf{r}\mathbf{r}'} Q_{\mathbf{r}} \mathcal{D}_{\mathbf{r}-\mathbf{r}'} Q'_{\mathbf{r}} - \sum_{\mathbf{r}} h_{\mathbf{r}} Q_{\mathbf{r}}$ and $Z^{tr} = \mathrm{Tr} e^{-\beta H^{tr}}$ its normalization. The Fourier transform of the function $\mathcal{D}_{\mathbf{r}-\mathbf{r}'}$ gives the frequency squared of the mode at wavevector $\mathbf{k}$, i.e., $\Omega_{\mathbf{k}}^2 = \sum_{\mathbf{r}\mathbf{r}'} \mathcal{D}_{\mathbf{r}\mathbf{r}'} e^{i\mathbf{k}\cdot(\mathbf{r}-\mathbf{r}')}$. $\Omega_{\mathbf{k}}^2$ is a variational function and it is determined by minimization of the free energy of the lattice degrees of freedom, $F_{\mathrm{lattice}} = \overline{\langle H \rangle} + T\overline{\langle k_B \ln \rho^{tr} \rangle}$. Here, $\overline{\langle .... \rangle}$ denotes thermal and compositional averages. The free energy per site is therefore given by,

$$\frac{F_{\mathrm{lattice}}}{N} = -\frac{\kappa}{2}\left(\frac{1}{N}\sum_{\mathbf{k}} \eta_{\mathbf{k}}\right) + \frac{3\gamma}{4}\left(\frac{1}{N}\sum_{\mathbf{k}} \eta_{\mathbf{k}}\right)^2 + \frac{1}{2N}\sum_{\mathbf{k}} V_{\mathbf{k}}(\phi_0)\,\eta_{\mathbf{k}} - \frac{1}{N}\sum_{\mathbf{k}} \frac{\Delta^2}{\Omega_{\mathbf{k}}^2} - \frac{1}{4N}\sum_{\mathbf{k}} \Omega_{\mathbf{k}} \coth\left(\frac{\beta\Omega_{\mathbf{k}}}{2}\right) + \frac{k_B T}{N}\sum_{\mathbf{k}} \ln\left[2\sinh\left(\frac{\beta\Omega_{\mathbf{k}}}{2}\right)\right], \tag{S8}$$

where $\eta_{\mathbf{k}} = \frac{1}{2\Omega_{\mathbf{k}}} \coth\left(\frac{\beta\Omega_{\mathbf{k}}}{2}\right) + \frac{\Delta^2}{\Omega_{\mathbf{k}}^4}$ are mean squared fluctuations averaged over compositional disorder at wavevector $\mathbf{k}$. N is the number of lattice sites and the summations run over the first Brillouin zone of the square lattice. Minimization of the free energy (S8) with respect to $\Omega_{\mathbf{k}}$ gives the following result,

$$\Omega_{\mathbf{k}}^2 = -\kappa + 3\gamma \frac{1}{N}\sum_{\mathbf{k}'} \left[\frac{1}{2\Omega_{\mathbf{k}'}} \coth\left(\frac{\beta\Omega_{\mathbf{k}'}}{2}\right) + \frac{\Delta^2}{\Omega_{\mathbf{k}'}^4}\right] + V_{\mathbf{k}}. \tag{S9}$$

Equation (S9) determines the temperature and disorder dependence of the mode frequency $\Omega_{\mathbf{k}}$ self-consistently.

III. MODEL PARAMETERS

Our model has six parameters ($\kappa, \gamma, a_D, a_S, a_T$, and $F_{\mathrm{Low\ T}}$), which are reduced to five as a_T (a_S) is combined with κ for the manganites (nickelates). We begin by choosing a set of of physically reasonable parameters which give phonon frequencies that are in order-of-magnitude agreement with the observed relevant modes.[S9,S10] We then take the resulting set of parameters and fine tune them to fit the observed dependence of T_c with the tolerance factor and compositional disorder. The resulting values are given in Table S1.

TABLE S1. Model parameters obtained from fits to the experiments in manganites and nickelates.[S11,S12] R is a rare earth element such as La, Pr, Nd, and Sm; and M is an alkaline earth metal such as Ca, Sr, Ba.

	κ [meV^2]	γ [meV^3]	a_D [meV^2]	a_S [meV^2]	a_T [meV^2]	$F_{\mathrm{Low\ T}}$ [meV]
$(R_{0.3}M_{0.7})MnO_3$	3.2×10^3	1.8×10^5	2.8×10^4	9.5×10^3	combined with κ	38
$RNiO_3$	7.1×10^3	6.02×10^5	4.3×10^4	combined with κ	2.1×10^4	78

[S1] T. F. Seman, K. H. Ahn, T. Lookman, A. Saxena, A. R. Bishop, and P. B. Littlewood, "Effects of rare-earth ion size on the stability of the coherent Jahn-Teller distortions in undoped perovskite manganites," Phys. Rev. B **86**, 184106 (2012).

[S2] K. H. Ahn, T. Lookman, and A. R. Bishop, "Strain-induced metal-insulator phase coexistance in perovskite manganites," Nature **428**, 401 (2004).

[S3] K. H. Ahn, T. Lookman, A. Saxena, and A. R. Bishop, "Atomic scale lattice distortions and domain wall profiles," Physical Review B **68**, 092101 (2003).

[S4] A. I. Larkin and S. A. Pikin, "Phase transitions of the first order but nearly of the second," Soviet Physics JETP **29**, 891 (1969).

[S5] S. Kartha, J. A. Krumhansl, J. P. Sethna, and L. K. Wickham, "Disorder-driven pretransitional tweed pattern in martensitic transformations," Phys. Rev. B **52**, 803 (1995).

[S6] K. H. Ahn, T. Lookman, A. Saxena, and A. R. Bishop, "Atomic scale lattice distortions and domain wall profiles," Physical Review B **68**, 092101 (2003).

[S7] M. Porta, T. Castán, P. Lloveras, T. Lookman, A. Saxena, and S. R. Shenoy, "Interfaces in ferroelastics: Fringing fields, microstructure, and size and shape effects," Phys. Rev. B **79**, 214117 (2009).

[S8] G. G. Guzmán-Verri, P. B. Littlewood, and C. M. Varma, "Paraelectric and ferroelectric states in a model for relaxor ferroelectrics," Phys. Rev. B **88**, 134106 (2013).

[S9] M. Zaghrioui, A. Bulou, P. Lacorre, and P. Laffez, "Electron diffraction and Raman scattering evidence of a symmetry breaking at the metal-insulator transition of $NdNiO_3$," Phys. Rev. B **64**, 081102 (2001).

[S10] L. Martín-Carrón, A. de Andrés, M. J. Martínez-Lope, M. T. Casais, and J. A. Alonso, "Raman phonons as a probe of disorder, fluctuations, and local structure in doped and undoped orthorhombic and rhombohedral manganites," Phys. Rev. B **66**, 174303 (2002).

[S11] L. M. Rodriguez-Martinez and J. P. Attfield, "Cation disorder and size effects in magnetoresistive manganese oxide perovskites," Phys. Rev. B **54**, R15622–R15625 (1996).

[S12] J. B. Torrance, P. Lacorre, A. I. Nazzal, E. J. Ansaldo, and Ch. Niedermayer, "Systematic study of insulator-metal transitions in perovskites $RNiO_3$ (R=Pr,Nd,Sm,Eu) due to closing of charge-transfer gap," Phys. Rev. B **45**, 8209–8212 (1992).